

Deep Comparison: Relation Columns for Few-Shot Learning

Xueting Zhang^{1*} Flood Sung^{2*} Yuting Qiang¹ Yongxin Yang¹ Timothy M. Hospedales¹
¹The University of Edinburgh ²Independent Researcher

{xueting.zhang, yongxin.yang, t.hospedales}@ed.ac.uk {floodsung, qianguyuting.new}@gmail.com

Abstract

Few-shot deep learning is a topical challenge area for scaling visual recognition to open-ended growth in the space of categories to recognise. A promising line work towards realising this vision is deep networks that learn to match queries with stored training images. However, methods in this paradigm usually train a deep embedding followed by a single linear classifier. Our insight is that effective general-purpose matching requires discrimination with regards to features at multiple abstraction levels. We therefore propose a new framework termed Deep Comparison Network (DCN) that decomposes embedding learning into a sequence of modules, and pairs each with a relation module. The relation modules compute a non-linear metric to score the match using the corresponding embedding module's representation. To ensure that all embedding module's features are used, the relation modules are deeply supervised. Finally generalisation is further improved by a learned noise regulariser. The resulting network achieves state of the art performance on both miniImageNet and tieredImageNet, while retaining the appealing simplicity and efficiency of deep metric learning approaches.

1. Introduction

The ability to learn from one or few examples is an important property of human learning that helps us to function effectively in the real world. Children learn new concepts effortlessly by building upon prior knowledge [3, 5]. In contrast, our most successful deep learning-based approaches to recognition [22, 15, 18] treat each learning problem as tabula-rasa, and as such are extremely data-inefficient compared to humans. This limits their scalability to open-ended learning of the long tail of categories in the real-world; and particularly their applicability to numerous real world problems where categories to recognise are rare (e.g., endangered species), continually emerging (man-made devices), or expensive to annotate (medical images).

These observations have motivated a resurgence of interest in few-shot learning in visual recognition [44, 9, 36, 32] and beyond [16, 7]. In the few-shot learning scenario, contemporary deep networks overfit – even when exploiting fine-tuning [45], data augmentation [22], or regularisation [38] techniques. The most effective few-shot methods rely on purpose built ‘meta-learning’ techniques, where transferable task-agnostic knowledge is extracted from historical tasks and leveraged to benefit sparse data learning of specific new target tasks. This task-agnostic knowledge here has taken several forms: Fast adaptation methods enable rapid adaptation using sparse data and without overfitting. For example good initial conditions [9] and learned optimisers [33]. Weight synthesis approaches learn a meta-network that inputs the training set and synthesizes weights for a recogniser [2, 28]. Deep metric learning approaches provide a robust way to represent [21] and compare [44, 36] instances allowing new categories to be recognised with nearest-neighbour style strategies. Existing methods each have different drawbacks, including complexity of inference mechanism [23], architectural complexity [23, 29], the need to fine-tune on the target problem [9, 33], or reliance on a simple linear comparison function [21, 44, 36].

We build on the ‘deep metric learning’ line of work due to its appealing architectural simplicity, and instantaneous training for new categories. These methods perform few-shot recognition by using auxiliary training tasks to learn a deep image-embedding such that the embedded data becomes linearly separable [21, 44, 36]. Thus the decision is non-linear in image-space, but linear in the embedding space. For learning the target task, few-shot training data is simply memorised. For testing the target task at runtime, query images are matched to training examples by applying the deep embedding and comparison function. Within this paradigm, the recently proposed RelationNet [40] achieved state-of-the-art performance by learning a *non-linear comparison function*. Learning the embedding and non-linear relation module jointly alleviates the reliance on the embedding’s ability to generate linearly separable features.

We build on this idea of jointly learning an embedding and non-linear comparison function, but take it further with

*Equal contribution.

the following insights. Different layers of deep networks represent different types of features at different levels of abstraction [47] – from simple textures to complex parts. A general purpose comparison network should be able to make use of any and all of these cues in making its decisions. Therefore we work with embedding networks composed of a sequence of modules, and pair each embedding module with its own non-linear comparison module. Thus resulting in a column of non-linear relation modules, where prior studies used a single linear [36], or non-linear comparison [40]. To provide the inductive bias that each layer of representation should be potentially discriminative for matching, and enable better gradient propagation [19] to each relation module, we deeply supervise [25] all the relation modules. Finally, since the hierarchy of added relation modules increases the parameter total, we develop a learned-noise stochastic regularizer to reduce overfitting and improve generalisation.

Overall our approach can be seen as jointly learning and embedding and comparison as the task-agnostic meta knowledge [21, 44, 36, 40], but extending this successful idea to make full use of deep networks by making comparison with the full feature hierarchy extracted by the embedding network. The resulting framework maintains the architectural simplicity and efficiency of other methods in this line, while providing state of the art performance on both the established *miniImageNet* benchmark, and the more challenging *tieredImageNet* few-shot learning benchmarks.

2. Related Work

Contemporary approaches to deep-network few-shot learning have exploited the learning-to-learn paradigm. Auxiliary tasks are used to meta-learn some task agnostic knowledge, before exploiting this to learn the target few-sample more effectively problem. The learning-to-learn idea has a long history [42, 8, 23], but contemporary approaches typically cluster into three categories: Fast adaptation, weight synthesis, and metric-learning approaches.

Fast Adaptation These approaches aim to meta-learn an optimisation process that enables base models to be fine-tuned quickly and robustly. So that a base model can updated for sparse data target problems without extensive overfitting. Effective ideas include the simply meta-learning an effective initial condition [9, 31], and learning a recurrent neural network optimizer to replace the standard SGD learning approach [33]. Recent extensions include also learning per-parameter learning rates [26], and accelerating fine-tuning through solving some layers in closed form [1]. Nevertheless, these methods suffer from needing to be fine-tuned for the target problem, often generating costly higher-order gradients during meta-learning, and failing [9] to scale to deeper network architectures as shown in [28]. They also

often suffer from a fixed parametric architecture. For example, once you train MAML [9] for 5-way auxiliary classification problems, it is restricted to the same for target problems without being straightforwardly generalizable to a different cardinality of classification.

Classifier Synthesis Another line of work focuses on synthesising a classifier based on the provided few-shot training data [12]. An early method in this line learned a transferable ‘LearnNet’ that generated convolutional weights for the base recognition network given a one-shot training example [2]. However, this was limited to binary classification. Conditional Neural Processes [12] exploited a similar idea, but in a Bayesian framework. SNAIL obtained excellent results by embedding the training set with temporal convolutions and attention [28]. Recently Qiao *et al.* proposed a method to predict classification parameters given neuron activations [32]. In this case the global parameter prediction network is the task-agnostic knowledge that is transferred from auxiliary categories. Compared to the fast adaptation approaches, these methods generally synthesize their classifier in a single pass, making them faster to train on the target problem. However learning to synthesize a full classifier does entail some complexity. This process can overfit and generalize poorly to novel target problem.

Deep Metric Learning These approaches aim to learn a deep embedding that extracts features that robustly describe instances, allowing them to be classified directly with nearest neighbour type strategies in the embedding space. The deep embedding forms the task agnostic knowledge that is transferred from auxiliary to target tasks. Early work simply used Siamese networks [21] to embed images, such that images of the same class are placed near each other. Matching networks [44] defined a differentiable nearest-neighbour loss based on cosine similarity between the support set and query embedding. Prototypical Networks [36] provide a simpler but more effective variant of this idea where the support set instances for one class are embedded as a single prototype. Their analysis showed that this leads to a linear classifier in the embedding space. The most related method to ours is RelationNet [40], which extended this line of work to use a separate non-linear comparison module instead of relying entirely on the embedding networks to make the data linearly separable [21, 36, 44]. This division of labour between a deep embedding and a deep relation module improved performance in practice [40]. Our approach builds on this line of work in general and RelationNet in particular. RelationNet relied on the embedding networks to produce a *single* embedding for the relation module to compare. We argue that a general purpose comparison function should use any or all of the full feature hierarchy [47] to make matching decisions. For example matching based on colors, textures, or parts – which may be represented at different layers in a embedding network. To this end we modularise the embed-

ding networks, and pair every embedding module with its own relation module.

Use of Feature Hierarchies The general strategy of simultaneously exploiting multiple layers of a feature hierarchy has been exploited in conventional many-shot classification network [19, 39], instance recognition [6], and semantic segmentation networks [13]. However, not to our knowledge in the context of deep-metric learning, where the conventional pipeline is to extract a complete feature [11, 17]. Importantly, in contrast to prior approaches’ single ‘short-cut’ connection of deeper features to a classifier [13, 6], we uniquely learn a hierarchy of relation modules: One non-linear comparison function for each block of the embedding. Our approach is also reminiscent of classic techniques such as spatial pyramids [24] (since each module in the hierarchy operates at different spatial resolutions) and multi-kernel learning [43] (since we learn multiple relation modules for each feature in the hierarchy).

Noise and Regularisation For best performance, we would like to fully exploit a state of the art embedding module architecture (we use SENet [18]), and also benefit from the array of comparison modules mentioned above. However the parameters introduced in such a rich architecture and multiple embedding modules introduce additional overfitting risk. We therefore develop a novel regularisation technique by adding learned Gaussian noise at each network module. Rather than generating deterministic features at a module output, we generate means and variances which are sampled in the forward pass, with backpropagation relying on the reparamaterisation trick. Unlike density networks [4] where such distributions are only generated at the output layer, or VAEs [20] here they are generated only once by the generator, we generate multiple such stochastic features at each embedding module’s output. This turns out to be an effective strategy for avoiding overfitting.

3. Methodology

3.1. Problem Definition

We consider a K -shot C -way classification problem for few shot learning. There are some labelled source tasks with sufficient data, denoted meta-train $\mathcal{D}_{m\text{-train}}$, and we ultimately want to solve a new set of target tasks denoted meta-test $\mathcal{D}_{m\text{-test}}$ (Fig. 1), for which the label space is disjoint. Within meta-train and meta-test, we denote each task as being composed of a support set of training examples, and a query set of testing examples. The meta-test tasks are assumed to be few-shot, so $\mathcal{D}_{m\text{-test}}$ contains a support set with C categories and K examples each. We want to learn a model on meta-train that can generalise out of the box, without fine-tuning, to learning the new categories in meta-test.

Episodic Training We adopt an episodic training

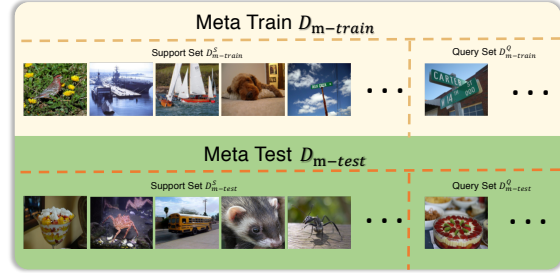


Figure 1: Few-shot learning: Problem Setup.

paradigm for few-shot meta-learning. During meta-training, an episode is formed as follows: (i) Randomly select C classes from $\mathcal{D}_{m\text{-train}}$, (ii) For each class, sample K images, which serve as *support set* $\mathcal{D}_{m\text{-train}}^S = \{(x_i, y_i)\}_{i=1}^m$, where $m = K * C$, (iii) For the same C classes, sample another set serving as the *query set* $\mathcal{D}_{m\text{-train}}^Q = \{(\tilde{x}_j, \tilde{y}_j)\}_{j=1}^n$, where $n = K' * C$ and $\mathcal{D}_{m\text{-train}}^S \cap \mathcal{D}_{m\text{-train}}^Q = \emptyset$. The support/query distinction mimics the $\mathcal{D}_{m\text{-test}}$ /real-time testing. Our few-shot DCN will be trained for instance comparison using episodes constructed in this manner.

3.2. Model

Overview Deep Comparison Network (DCN) is composed of two module types: *embedding* and *relation* modules, as shown in Fig. 2. The detailed architecture will be given in Section 3.3. A pair of images x_i and x_j in the support and query respectively set are fed to embedding modules. The v th-level of embedding modules produce feature maps $f_\theta^v(x_i)$ and $f_\theta^v(x_j)$, which are concatenated $[f_\theta^v(x_i), f_\theta^v(x_j)]$, and then fed into the corresponding, i.e., v th-level, relation module.

For the pair of x_i and x_j , at level v , the relation module outputs a similarity feature map g_ϕ^v . Each relation module also inputs the similarity feature map of the previous relation module in the hierarchy,

$$g_\phi^v = g([f_\theta^v(x_i), f_\theta^v(x_j)], g_\phi^{v-1}). \quad (1)$$

The first relation module is special as it does not have a predecessor to input, and we can not use zero-padding because 0 has a specific meaning in our context, thus we set $g_\phi^1 = g([f_\theta^1(x_i), f_\theta^1(x_j)])$.

Simultaneously, after an average pooling and fully connected layer denoted q , each relation module outputs a real-valued scalar in the range of $[0, 1]$, representing the v th-level similarity/relation score $r_{i,j}^v$ of two images,

$$r_{i,j}^v = q(g_\phi^v). \quad (2)$$

K-Shot For K -shot with $K > 1$, the embedding module outputs the average pooling of features, along the sample

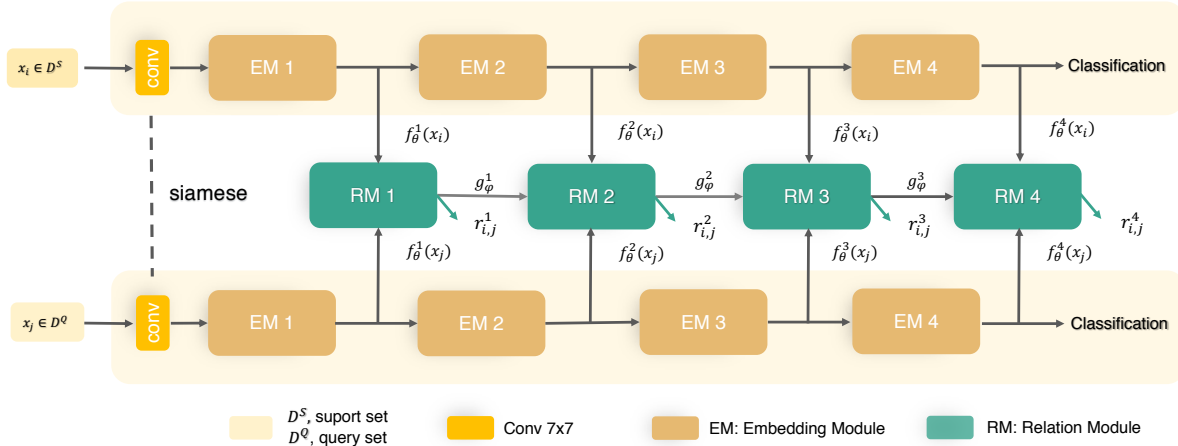


Figure 2: Deep Comparison Network architecture. There are 4 embedding modules for each embedding branch, and a set of 4 corresponding relation modules.

axis, of all samples from the same class to produce *one* feature map. Thus, the number of outputs for the v -level relation module is C , regardless of the value of K .

Objective Function We train the Siamese embedding networks as a conventional multi-class classifier for the classes in $\mathcal{D}_{m-\text{train}}$ using cross entropy (CE) loss. After training, the embedding module parameter θ is fixed.

Binary cross entropy (BCE) loss is then used to train the column of relation modules, with one loss applied to each of the four modules (Fig. 2). Since we have multiple relation modules, we can assign different weights, $[w_1, w_2, \dots, w_V], v = 1, 2, \dots, V$ to different modules,

$$\phi \leftarrow \underset{\phi}{\operatorname{argmin}} \sum_{v=1}^V w_v \operatorname{BCE}(r_{i,j}^v, \mathbf{1}(y_i = y_j)). \quad (3)$$

Testing Strategy To evaluate our learned model on C -way- k -shot learning, we calculate the final relation score r_c of query images to different classes using the same weight assignment as the weighted sum loss $[w_1, w_2, \dots, w_V], v = 1, 2, \dots, V$, as shown in Eq. 4. The class with the highest relation score r_c is the final predicted classification.

$$r_c = \sum_{v=1}^V \omega_v \cdot r_{i,j}^v. \quad (4)$$

3.3. Network Architecture

The Deep Comparison Network architecture (Fig. 2) uses 4 embedding modules, each paired with a relation module.

Embedding Subnetwork As shown in Fig. 2, first we use a 7×7 convolution followed by a 3×3 max-pooling for size reduction. Then, we have 4 embedding modules, each composed of a number of SENet [18] blocks. Finally, an

avg-pooling and a fully-connected layer are used to produce C' logit values, corresponding to C' classes in $\mathcal{D}_{m-\text{train}}$.

More specifically, the embedding modules [1, 2, 3, 4] have [3, 4, 6, 3] SENet blocks respectively, as per [18]. Empirically, we found that SENet blocks achieved the best performance compared to conventional convolutional blocks, WRN blocks [46], and ResNet blocks [15]. We use exactly the same configuration of SENet block as proposed in [18], e.g., reduction ratio $r = 16$ as suggested.

Parameterized Gaussian Noise for Stochastic Feature Regularisation Conventionally, an embedding module outputs deterministic features. As a regularisation strategy, we treat each feature output as a random variable drawn from a parameterized Gaussian distribution, for which the embedding module outputs the mean and variance. This design is illustrated in Fig. 3.

To realise this idea, each embedding module's output is split into two parts: the mean feature $f_{\theta,\mu}$ sized $[b, c, h, w]$ ([batch_size, channel, height, width]), and standard deviation $f_{\theta,\sigma}$ sized $[b, 1, h, w]$. Note that we assume that every channel shares the same standard deviation (std). This means, in addition to the penultimate-to-output layer (now it is penultimate-to-mean layer), we have a new penultimate-to-std layer (with its own parameters). The motivation behind sharing the std across channels is to reduce the number of parameters in that newly introduced layer. We also control the amount of noise added by constraining the standard deviation to the range $[0, 1]$ by applying sigmoid activation.

To generate the final output, we draw one (or more) random sample from the Gaussian distribution. However, the conventional sampling process is not differentiable, thus we use the reparameterization trick,

$$f_{\theta,\mu} + \varepsilon \odot f_{\theta,\sigma}, \quad (5)$$

Output size	Embedding	Embedding+ noise	Output size	Relation
112 × 112	conv, 7 × 7, 64, stride 2, padding 3			
56 × 56	Maxpooling 3 × 3, stride 2, padding 1			
56 × 56	$\begin{bmatrix} \text{conv}, 3 \times 3, 64 \\ \text{conv}, 3 \times 3, 64 \\ \text{fc}, [4, 64] \end{bmatrix} \times 3$	$\begin{bmatrix} \text{conv}, 3 \times 3, 64 \\ \text{conv}, 3 \times 3, 64 \\ \text{fc}, [4, 64] \end{bmatrix} \times 2$ $\begin{bmatrix} \text{conv}, 3 \times 3, 64 \\ \text{conv}, 3 \times 3, 65 \\ \text{fc}, [4, 65] \end{bmatrix} \times 1$	28 × 28	$\begin{bmatrix} \text{conv}, 3 \times 3, 128 \\ \text{conv}, 3 \times 3, 128 \\ \text{fc}, [8, 128] \end{bmatrix} \times 2$
28 × 28	$\begin{bmatrix} \text{conv}, 3 \times 3, 128 \\ \text{conv}, 3 \times 3, 128 \\ \text{fc}, [8, 128] \end{bmatrix} \times 4$	$\begin{bmatrix} \text{conv}, 3 \times 3, 128 \\ \text{conv}, 3 \times 3, 128 \\ \text{fc}, [8, 128] \end{bmatrix} \times 3$ $\begin{bmatrix} \text{conv}, 3 \times 3, 128 \\ \text{conv}, 3 \times 3, 129 \\ \text{fc}, [8, 129] \end{bmatrix} \times 1$	14 × 14	$\begin{bmatrix} \text{conv}, 3 \times 3, 384 \\ \text{conv}, 3 \times 3, 256 \\ \text{fc}, [16, 256] \end{bmatrix} \times 1$ $\begin{bmatrix} \text{conv}, 3 \times 3, 256 \\ \text{conv}, 3 \times 3, 256 \\ \text{fc}, [16, 256] \end{bmatrix} \times 1$
14 × 14	$\begin{bmatrix} \text{conv}, 3 \times 3, 256 \\ \text{conv}, 3 \times 3, 256 \\ \text{fc}, [16, 256] \end{bmatrix} \times 6$	$\begin{bmatrix} \text{conv}, 3 \times 3, 256 \\ \text{conv}, 3 \times 3, 256 \\ \text{fc}, [16, 256] \end{bmatrix} \times 5$ $\begin{bmatrix} \text{conv}, 3 \times 3, 256 \\ \text{conv}, 3 \times 3, 257 \\ \text{fc}, [16, 257] \end{bmatrix} \times 1$	7 × 7	$\begin{bmatrix} \text{conv}, 3 \times 3, 768 \\ \text{conv}, 3 \times 3, 512 \\ \text{fc}, [32, 512] \end{bmatrix} \times 1$ $\begin{bmatrix} \text{conv}, 3 \times 3, 512 \\ \text{conv}, 3 \times 3, 512 \\ \text{fc}, [32, 512] \end{bmatrix} \times 1$
7 × 7	$\begin{bmatrix} \text{conv}, 3 \times 3, 512 \\ \text{conv}, 3 \times 3, 512 \\ \text{fc}, [32, 512] \end{bmatrix} \times 3$	$\begin{bmatrix} \text{conv}, 3 \times 3, 512 \\ \text{conv}, 3 \times 3, 512 \\ \text{fc}, [32, 512] \end{bmatrix} \times 2$ $\begin{bmatrix} \text{conv}, 3 \times 3, 512 \\ \text{conv}, 3 \times 3, 513 \\ \text{fc}, [32, 513] \end{bmatrix} \times 1$	7 × 7	$\begin{bmatrix} \text{conv}, 3 \times 3, 1536 \\ \text{conv}, 3 \times 3, 512 \\ \text{fc}, [32, 512] \end{bmatrix} \times 1$ $\begin{bmatrix} \text{conv}, 3 \times 3, 512 \\ \text{conv}, 3 \times 3, 512 \\ \text{fc}, [32, 512] \end{bmatrix} \times 1$
1 × 1	Global average pooling, fc			

Table 1: Parameters of each embedding (conventional and noise-generating) and relation module. Relation modules concatenate the final feature maps of both corresponding embedding modules, and the previous relation module. The output size of each embedding module matches the input size of the corresponding relation module. The brackets of ‘fc’ indicate the dimension of FC layers in an SE block [18].

where ε is $b \times 1 \times h \times w$ random samples drawn from a standard Gaussian and reshaped into $[b, 1, h, w]$; \odot denotes element-wise product; and we perform broadcasting across the channels using the shared std.

Relation Subnetwork As illustrated in Fig. 2, the relation column consists of 4 serial modules, each of which has 2 SENet blocks. They each finish with a pooling, and fully-connected layer to produce the relation score. The SENet block architecture is the same as the one used in embedding module. The detailed relation module architectures are shown in Tab. 1. In Eq. 3, we have the weighting terms for each sub-module’s loss, and we fix them to be [0.3, 0.4, 0.5, 1.0]. This increasing pattern reflects the expectation that later layers are generally more discriminative, and the aggregation effect of the column structure passing feature maps between relation modules (Eq. 2).

4. Experiments

Our approach is evaluated on few-shot classification using two datasets: *miniImagenet* and *tieredImagenet*.

Baselines We compare against several state of the art baselines for few-shot learning including Matching Nets [44], Meta Nets [29], Meta LSTM [33], MAML [9], Prototypical Nets [36], Graph Neural Nets [10], Relation Net [40], Meta-SGD [26], SNAIL [28], DynamicFSL [12], AdaResNet [30], Meta-SSL [34], PPA [32] and TPN [27].

Data Augmentation We follow the standard data augmentation [41] with random-size cropping to 224*224 pixels and random horizontal flipping. Input images are normalized through mean channel subtraction.

Pre-train and Retrain We firstly pre-train the supervised feature embedding branch using the training set and then fix the parameters of embedding sub-network, before meta-training the relation sub-network. We then use the validation set to estimate the right number of early stop episodes for

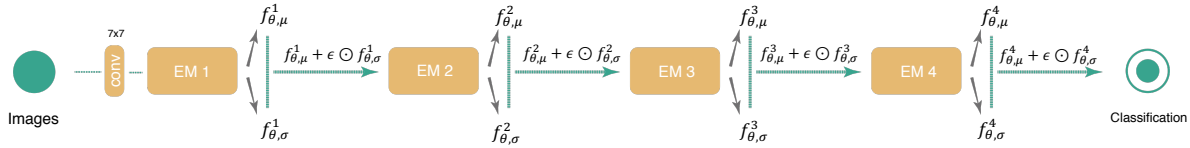


Figure 3: Learned noise regularizer: Each embedding module defines a Gaussian distribution from which its output feature is sampled.

the relation training. Finally, we use all 80 train+validation classes (as per common practice [32]) to retrain both the embedding and relation sub-networks.

4.1. *miniImageNet*

Dataset *miniImageNet* consists of 100 ImageNet classes, each with 600 images (60,000 colour images in total) [44]. Following the split in [33], the dataset is divided into a 64-class training set, 16 validation and a 20-class testing set.

Settings We evaluate both *5-way-1-shot* and *5-way-5-shot*. In both settings, each episode contains 5 query images for each of the C sampled classes. Thus, there are $5 \times 5 + 1 \times 5 = 30$ images per training episode/mini-batch for *5-way-1-shot* experiments, and $5 \times 5 + 5 \times 5 = 50$ images for *5-way-5-shot* experiments. In terms of *5-way-5-shot* learning, recall that we calculate the class-wise average feature across the support set. Thus we always get $5 \times 5 \times 5 \times 1 = 75$ feature pairs as input for the relation module.

For embedding and relation module training, optimization uses SGD with momentum 0.9. The initial learning rate is 0.1, decreased by a factor of 5 every 60 epochs, and the training epoch is 200. All models are trained from scratch, using the robust RELU weight initialisation [14]. For testing, we resize shorter image edges to 256, and evaluate on 224×224 central pixels cropped from each image.

Results Following the settings of [36], when evaluating testing performance, we batch 15 query images per class in a testing episode and the accuracy is calculated by averaging over 600 randomly generated testing tasks (for both both 1-shot and 5-shot scenarios). From Tab. 2, we can see that DCN achieves the new state-of-the-art performance on the *5-way-1-shot* and *5-shot* tasks with comfortable margins. Specifically, the accuracy of testing on *5-way miniImageNet* reaches 62.88% and 75.84% for 1-shot and 5-shot respectively. This improves by 3.3% and 2.1% respectively on prior state of the art method PPA [32]. Note that Tab. 2 divides competitors into those that use relatively shallow image embeddings (top) with those that use state-of-the-art deep architectures (bottom).

Cross-way Testing Results Standard procedure in few-shot evaluation is to train models for the desired number of categories to discriminate at testing time. However unlike alternatives such as MAML [9], our method is not required

Model	<i>miniImageNet</i> 5-way Acc.	
	1-shot	5-shot
MATCHING NETS [44]	43.56 ± 0.84%	55.31 ± 0.73%
META LSTM [33]	43.44 ± 0.77%	60.60 ± 0.71%
MAML [9]	48.70 ± 1.84%	63.11 ± 0.92%
META NETS [29]	49.21 ± 0.96%	-
PROTOTYPICAL NETS [36]	49.42 ± 0.78%	68.20 ± 0.66%
GNN [10]	50.33 ± 0.36%	66.41 ± 0.63%
META SSL [34]	50.41 ± 0.31%	64.39 ± 0.24%
RELATION NET [40]	50.44 ± 0.82%	65.32 ± 0.70%
META SGD [26]	50.47 ± 1.87%	64.03 ± 0.94%
TPN [27]	52.78 ± 0.27%	66.59 ± 0.28%
SNAIL [35]	55.71 ± 0.99%	68.88 ± 0.92%
DYNAMIC FSL [12]	56.20 ± 0.86%	73.00 ± 0.64%
ADARESNET [30]	57.10 ± 0.70%	70.04 ± 0.63%
PPA [32]	59.60 ± 0.41%	73.74 ± 0.19%
DEEP COMPARISON NETWORK	62.88 ± 0.83%	75.84 ± 0.65%

Table 2: Few-shot classification results on *miniImageNet*. All accuracies are averaged over 600 test episodes and are reported with 95% confidence intervals. For each task, the best-performing method is bold, along with any others whose confidence intervals overlap. ‘-’: not reported.

Model	<i>miniImageNet</i> 20-way Acc.	
	1-shot	5-shot
MATCHING NETS, (from [26])	17.31 ± 0.22%	22.69 ± 0.86%
META LSTM, (from [26])	16.70 ± 0.23%	26.06 ± 0.25%
MAML, (from [26])	16.49 ± 0.58%	19.29 ± 0.29%
META SGD [26]	17.56 ± 0.64%	28.92 ± 0.35%
DEEP COMPARISON NETWORK	32.07 ± 0.29%	47.31 ± 0.25%

Table 3: 20-way classification accuracy on *miniImageNet*. Our DCN is trained for 5-way and transferred to 20-way. Meta LSTM, MAML, and Meta SGD results are from [26].

to match label cardinality between training and testing. We therefore evaluate our *5-way* trained model on *20-way* testing in Tab. 3. We can see that our model outperforms the alternatives clearly despite DCN being trained for *5-way*, and the others specifically for *20-way*. This demonstrates another important aspect of DCN’s flexibility and general applicability.

Model	<i>tieredImageNet</i> 5-way Acc.	
	1-shot	5-shot
REPTILE, (from [27])	48.97%	66.47%
MAML, (from [27])	51.67%	70.30%
META SSL [†] [34]	52.39 ± 0.44%	70.25 ± 0.31%
PROTOTYPICAL NET, (from [27])	53.31%	72.69%
RELATION NET, (from [27])	54.48%	71.31%
TPN [†] [27]	59.91%	73.30%
DEEP COMPARISON NETWORK	68.83 ± 0.94%	79.62 ± 0.77%

Table 4: Few-shot classification results on *tieredImageNet*. All accuracies are averaged over 600 test episodes and reported with 95% confidence intervals. For each task, the best-performing method is bold. [†] Indicates methods that make use of additional unlabeled data for semi-supervised learning or transductive inference.

4.2. *tieredImageNet*

Dataset *tieredImageNet* is a newer and larger few-shot recognition benchmark than *miniImageNet*. It contains 608 classes (779,165 images), and the training/validation/testing categories are organized so as to ensure a larger semantic gap than those in *miniImageNet*, thus providing a more rigorous test of generalisation. This is achieved by dividing according to 34-higher-level nodes in the ImageNet hierarchy [34]. These 34 broad categories are grouped into 20 for training (351 classes), 6 for validation (97 classes) and 8 for testing (160 classes).

Settings Similar to the setting of *miniImageNet*, we use 5 query images per training episode. In terms of training the embedding modules, due to the larger data size, we use a larger batch size 512, initial learning rate 0.3 and 100 training epochs. Other settings remain the same.

Results Following the former experiments, we batch 15 query images per class in each testing episode for both 1-shot and 5-shot scenarios, and the accuracy is calculated by averaging over 600 randomly generated testing tasks. From Tab. 4, DCN achieves the new state-of-the-art performance on the 5-way-1-shot and 5-shot tasks with comfortable margins. Specifically, the testing accuracy on *tieredImageNet* reaches 68.83% and 79.62% for 5-way-1-shot and 5-way-5-shot respectively. This is a clear 8.92% and 6.32% improvements on prior state of the art TPN [27]. We note also that state-of-the-art competitors Meta-SSL [34] and TPN [27] are semi-supervised methods that use more information than ours, and have additional requirements such as access to the test set for transduction.

4.3. Further Analysis

4.3.1 Ablation Study

Our experiments demonstrate that our approach outperforms prior state-of-the-art by a large margin. To investigate the

contribution of the different components of our method, we conduct a series of ablation studies reported in Tab. 5. The conclusions are as follows: **Gaussian Noise:** Comparing DCN and DCN-No Noise, we can see that this brings just over 2% improvement. **Retraining:** The impact of retraining on the combined training and validation set is visible by comparing the entries with DCN-No Retrain. Retraining provides a similar 2% margin, and this is complementary to the noise. **Deep Supervision:** From the DCN-No Deep Sup. result, we can see that deep supervision is important to gain full benefit from the column of relation modules. **Architecture:** From the results we can see that our DCN benefits from deeper embedding architectures. It from using the simple convolutional blocks used by early studies [9, 36, 40] when equipped with ResNet [15], Wide Res Net [46] and SENet [18]. Nevertheless when fixing a common SimpleConv embedding for comparing all models, DCN outperforms the alternatives MAML [9], RelationNet [40] and Prototypical Nets [36], as well as other prior methods with simple embeddings (upper block, Tab. 2). In contrast, when fixing a common SENet embedding, the related and recently state of the art method RelationNet [40] improves, but is still surpassed by DCN. It is also important to note that improvements from deeper embeddings are not automatic. Competitors PrototypicalNet [36] (evaluated by us) and MAML [9] (evaluated by [28]) failed to benefit from deeper embeddings, actually overfitting and becoming worse. **Multiple Relation Modules:** Finally, we also compare separately the testing accuracy with each DCN relation module output score r_v in isolation (DCN_ r_v). We can see that each individual module performs competitively, but their combination clearly leads to the best overall performance, supporting our argument that multiple levels of the feature hierarchy should be used to make general purpose matching decisions.

4.3.2 Relation Module Analysis

A key contribution of our model is to perform metric learning at multiple abstraction levels simultaneously via a series of paired relation and embedding modules. We now analyse the differences between relation modules to provide some insight into their complementarity. **Score-Distance Correlation** We first checked how the relation module (RM) scores relate to distances in the ImageNet hierarchy. Using *miniImageNet* data, we searched for (*support1, support2, query*) category tuples where the distance $D(query, support1)$ and $D(query, support2)$ matched a certain number of links, and then plotted instances from these tuples query categories against the relative relation module scores $RM(q, s1)$, $RM(q, s2)$. Fig. 4 presents scatter plots for the four relation modules where points are images and colors indicate category tuples with specified distance from the two support classes. We can see that: (1) The

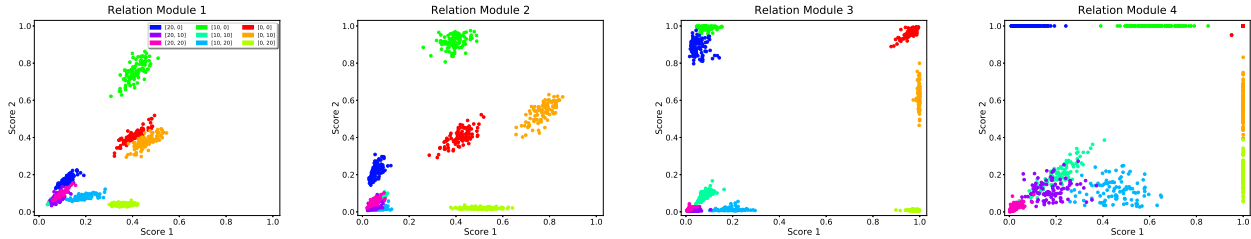


Figure 4: Illustration of query-support score distribution and the link to ImageNet hierarchy. Colors indicate query images of a (*query*, *support1*, *support2*) class triple matching the specified ImageNet distance relationship $[D(q, s1), D(q, s2)]$.

Model	<i>miniImageNet</i> Acc.
	5-way 1-shot
DCN Our full model	62.88 ± 0.83%
DCN-No noise	60.57 ± 0.86%
DCN-No retrain	60.79 ± 0.88%
DCN-No retrain, No noise	58.04 ± 0.82%
DCN-No deep sup.	58.02 ± 0.80%
DCN + SimpleConv	53.48 ± 0.78%
DCN + ResNet	60.24 ± 0.82%
DCN + WRN	57.28 ± 0.81%
DCN + SENet	62.88 ± 0.83%
RELATION NET [40] + SimpleConv	50.44 ± 0.82%
RELATION NET [40] + SENet	57.39 ± 0.86%
PROTOTYPICAL [36] + SimpleConv	49.42 ± 0.78%
PROTOTYPICAL [36] + SENet	47.61 ± 0.82%
MAML [9] + SimpleConv	48.70 ± 1.84%
MAML [9] + Deep [28]	30.10%
DCN- r_1	52.25 ± 0.80%
DCN- r_2	58.07 ± 0.80%
DCN- r_3	60.69 ± 0.81%
DCN- r_4	58.31 ± 0.79%

Table 5: Ablation study using 5-way-1-shot classification on *miniImageNet*.

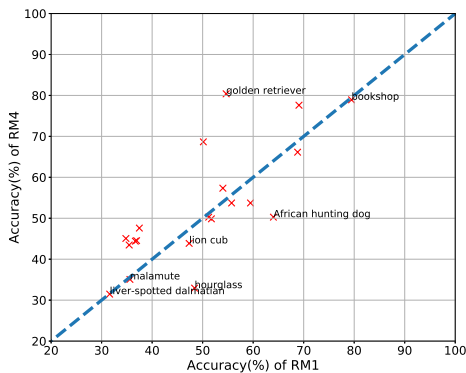


Figure 5: Category-wise accuracy of RM1 vs RM4.

scores generally match ImageNet distances: The most/least similar categories (red/magenta) are usually closer to the top right/bottom left of the plot; while query categories closer to

Module	RM1	RM2	RM3	RM4
RM1	-	-	-	-
RM2	0.75	-	-	-
RM3	0.55	0.73	-	-
RM4	0.34	0.45	0.61	-

Table 6: Spearman rank-order correlation coefficient between different relation modules.

one support class are in the opposite corners (blue/yellow-green). (2) Generally higher numbered relation modules are more discriminative, separating classes with larger differences in relation score.

Score Correlation We next investigated if relation module predictions are diverse or redundant. We analysed the correlation in their predictions by randomly picking 10,000 image pairs from *miniImageNet* and computing the Spearman rank-order correlation coefficient [37] between each pair of relation module’s scores. The results in Tab. 6, show that: (1) Many correlations are relatively low (down to 0.34), indicating that they are making diverse, non-redundant predictions; and (2) Adjacent RMs have higher correlation than non-adjacent RMs, indicating that prediction diversity is related to RM position in the feature hierarchy.

Prediction Success by Module We know that RM predictions do not necessarily agree. But to find out if they are complementary, we made a scatter plot of the per-class accuracy of RM-1 vs RM-4 in Fig. 5. We can see that many categories lie on the diagonal, indicating that RM-1 and-4 get them right equally often. However there are some categories *below* the diagonal, indicating that RM-1 gets them right more often than RM-4. Examples include both stereotyped and fine-grained categories such as ‘hourglass’ and ‘African hunting dog’. These below diagonal elements confirm the value of using deeper features in metric learning.

5. Conclusion

We proposed Deep Comparison Networks, a new general purpose matching framework for few-shot learning. This architecture performs effective few-shot learning via learning

non-linear comparisons simultaneously at multiple levels of feature extraction, while resisting overfitting. The resulting method achieves state of the art results on *miniImageNet* and the more ambitious *tieredImageNet*, while retaining architectural simplicity, and fast training and testing processes.

References

- [1] L. Bertinetto, J. F. Henriques, P. H. Torr, and A. Vedaldi. Meta-learning with differentiable closed-form solvers. *arXiv preprint arXiv:1805.08136*, 2018. [2](#)
- [2] L. Bertinetto, J. F. Henriques, J. Valmadre, P. H. S. Torr, and A. Vedaldi. Learning feed-forward one-shot learners. In *NIPS*, 2016. [1](#), [2](#)
- [3] I. Biederman. Recognition-by-components: A theory of human image understanding. *Psychological Review*, 94(2):115–147, 1987. [1](#)
- [4] C. M. Bishop. Mixture density networks. Technical report, Aston University, 1994. [3](#)
- [5] S. Carey and E. Bartlett. Acquiring a single new word. *Papers and Reports on Child Language Development*, (15):17–29, 1978. [1](#)
- [6] X. Chang, T. M. Hospedales, and T. Xiang. Multi-level factorisation net for person re-identification. In *CVPR*, 2018. [3](#)
- [7] Y. Duan, M. Andrychowicz, B. Stadie, O. J. Ho, J. Schneider, I. Sutskever, P. Abbeel, and W. Zaremba. One-shot imitation learning. In *NIPS*, 2017. [1](#)
- [8] L. Fei-Fei, R. Fergus, and P. Perona. One-shot learning of object categories. *TPAMI*, 2006. [2](#)
- [9] C. Finn, P. Abbeel, and S. Levine. Model-agnostic meta-learning for fast adaptation of deep networks. In *ICML*, 2017. [1](#), [2](#), [5](#), [6](#), [7](#), [8](#)
- [10] V. Garcia and J. Bruna. Few-shot learning with graph neural networks. In *ICLR*, 2018. [5](#), [6](#)
- [11] W. Ge, W. Huang, D. Dong, and M. R. Scott. Deep metric learning with hierarchical triplet loss. In *ECCV*, 2018. [3](#)
- [12] S. Gidaris and N. Komodakis. Dynamic few-shot visual learning without forgetting. In *CVPR*, 2018. [2](#), [5](#), [6](#)
- [13] B. Hariharan, P. Arbelaez, R. Girshick, and J. Malik. Hypercolumns for object segmentation and fine-grained localization. In *CVPR*, 2015. [3](#)
- [14] K. He, X. Zhang, S. Ren, and J. Sun. Delving deep into rectifiers: Surpassing human-level performance on imagenet classification. In *ICCV*, 2015. [6](#)
- [15] K. He, X. Zhang, S. Ren, and J. Sun. Deep residual learning for image recognition. In *CVPR*, 2016. [1](#), [4](#), [7](#)
- [16] A. Herbelot and M. Baroni. High-risk learning: acquiring new word vectors from tiny data. In *EMNLP*, 2017. [1](#)
- [17] J. Hu, J. Lu, and Y.-P. Tan. Discriminative deep metric learning for face verification in the wild. In *CVPR*, 2014. [3](#)
- [18] J. Hu, L. Shen, and G. Sun. Squeeze-and-excitation networks. In *CVPR*, 2018. [1](#), [3](#), [4](#), [5](#), [7](#)
- [19] G. Huang, Z. Liu, L. Van Der Maaten, and K. Q. Weinberger. Densely connected convolutional networks. In *CVPR*, 2017. [2](#), [3](#)
- [20] D. P. Kingma and M. Welling. Auto-encoding variational bayes. In *ICLR*, 2014. [3](#)
- [21] G. Koch, R. Zemel, and R. Salakhutdinov. Siamese neural networks for one-shot image recognition. In *ICML Deep Learning Workshop*, 2015. [1](#), [2](#)
- [22] A. Krizhevsky, I. Sutskever, and G. E. Hinton. Imagenet classification with deep convolutional neural networks. In *NIPS*, 2012. [1](#)
- [23] B. M. Lake, R. Salakhutdinov, and J. B. Tenenbaum. Human-level concept learning through probabilistic program induction. *Science*, 2015. [1](#), [2](#)
- [24] S. Lazebnik, C. Schmid, and J. Ponce. Beyond bags of features: Spatial pyramid matching for recognizing natural scene categories. In *CVPR*, 2006. [3](#)
- [25] C.-Y. Lee, S. Xie, P. W. Gallagher, Z. Zhang, and Z. Tu. Deeply-supervised nets. In *AISTATS*, 2015. [2](#)
- [26] Z. Li, F. Zhou, F. Chen, and H. Li. Meta-sgd: Learning to learn quickly for few shot learning. *arXiv preprint arXiv:1707.09835*, 2017. [2](#), [5](#), [6](#)
- [27] Y. Liu, J. Lee, M. Park, S. Kim, and Y. Yang. Transductive propagation network for few-shot learning. *arXiv preprint arXiv:1805.10002*, 2018. [5](#), [6](#), [7](#)
- [28] N. Mishra, M. Rohaninejad, X. Chen, and P. Abbeel. A simple neural attentive meta-learner. In *ICLR*, 2018. [1](#), [2](#), [5](#), [7](#), [8](#)
- [29] T. Munkhdalai and H. Yu. Meta networks. In *ICML*, 2017. [1](#), [5](#), [6](#)
- [30] T. Munkhdalai, X. Yuan, S. Mehri, and A. Trischler. Rapid adaptation with conditionally shifted neurons. In *ICML*, 2018. [5](#), [6](#)
- [31] A. Nichol, J. Achiam, and J. Schulman. On first-order meta-learning algorithms. *arXiv preprint arXiv:1803.02999*, 2018. [2](#)
- [32] S. Qiao, C. Liu, W. Shen, and A. L. Yuille. Few-shot image recognition by predicting parameters from activations. In *CVPR*, 2018. [1](#), [2](#), [5](#), [6](#)
- [33] S. Ravi and H. Larochelle. Optimization as a model for few-shot learning. In *ICLR*, 2017. [1](#), [2](#), [5](#), [6](#)
- [34] M. Ren, E. Triantafillou, S. Ravi, J. Snell, K. Swersky, J. B. Tenenbaum, H. Larochelle, and R. S. Zemel. Meta-learning for semi-supervised few-shot classification. In *ICLR*, 2018. [5](#), [6](#), [7](#)
- [35] A. Santoro, D. Raposo, D. G. Barrett, M. Malinowski, R. Pascanu, P. Battaglia, and T. Lillicrap. A simple neural network module for relational reasoning. In *NIPS*, 2017. [6](#)
- [36] J. Snell, K. Swersky, and R. S. Zemel. Prototypical networks for few-shot learning. In *NIPS*, 2017. [1](#), [2](#), [5](#), [6](#), [7](#), [8](#)
- [37] C. Spearman. The proof and measurement of association between two things. *The American Journal of Psychology*, 15(1):72–101, 1904. [8](#)
- [38] N. Srivastava, G. Hinton, A. Krizhevsky, I. Sutskever, and R. Salakhutdinov. Dropout: a simple way to prevent neural networks from overfitting. *JMLR*, 2014. [1](#)
- [39] R. K. Srivastava, K. Greff, and J. Schmidhuber. Highway networks. In *ICML Deep Learning Workshop*, 2015. [3](#)
- [40] F. Sung, Y. Yang, L. Zhang, T. Xiang, P. H. Torr, and T. M. Hospedales. Learning to compare: Relation network for few-shot learning. In *CVPR*, 2018. [1](#), [2](#), [5](#), [6](#), [7](#), [8](#)

- [41] C. Szegedy, W. Liu, Y. Jia, P. Sermanet, S. Reed, D. Anguelov, D. Erhan, V. Vanhoucke, and A. Rabinovich. Going deeper with convolutions. In *CVPR*, 2015. 5
- [42] S. Thrun. Is learning the n-th thing any easier than learning the first? In *NIPS*, 1996. 2
- [43] A. Vedaldi, V. Gulshan, M. Varma, and A. Zisserman. Multiple kernels for object detection. In *ICCV*, 2009. 3
- [44] O. Vinyals, C. Blundell, T. Lillicrap, D. Wierstra, et al. Matching networks for one shot learning. In *NIPS*, 2016. 1, 2, 5, 6
- [45] J. Yosinski, J. Clune, Y. Bengio, and H. Lipson. How transferable are features in deep neural networks? In *NIPS*, 2014. 1
- [46] S. Zagoruyko and N. Komodakis. Wide residual networks. In *BMVC*, 2016. 4, 7
- [47] M. D. Zeiler and R. Fergus. Visualizing and understanding convolutional networks. In *ECCV*, 2014. 2